THE JOURNAL OF BIOLOGICAL CHEMISTRY VOL. 288, NO. 20, pp. 14158–14169, May 17, 2013

Protein Kinase A Regulates MYC Protein through Transcriptional and Post-translational Mechanisms in a Catalytic Subunit Isoform-specific Manner*[S]

Received for publication, October 30, 2012, and in revised form, March 11, 2013 Published, JBC Papers in Press, March 15, 2013, DOI 10.1074/jbc.M112.432377

Achuth Padmanabhan[‡1], **Xiang Li**[‡], **and Charles J. Bieberich**[‡§2]

From the [‡]*Department of Biological Sciences, the University of Maryland Baltimore County, Baltimore, Maryland 21250 and the* [§]*Marlene and Stewart Greenebaum Cancer Center, University of Maryland, Baltimore, Maryland 21201*

Background: MYC is rapidly degraded in cells, and its accumulation is associated with many human malignancies.
Results: Sequential phosphorylation of MYC by protein kinase A (PKA) and polo-like kinase 1 (PLK1) protects MYC from proteasome-mediated degradation.
Conclusion: A MYC-PKA-PLK1 signaling loop exists in cells.
Significance: We highlight the importance of considering possible regulatory feedback loops while targeting molecules occupying hub positions in signaling pathways.

MYC levels are tightly regulated in cells, and deregulation is associated with many cancers. In this report, we describe the existence of a MYC-protein kinase A (PKA)-polo-like kinase 1 (PLK1) signaling loop in cells. We report that sequential MYC phosphorylation by PKA and PLK1 protects MYC from proteasome-mediated degradation. Interestingly, short term pan-PKA inhibition diminishes MYC level, whereas prolonged PKA catalytic subunit *α* (PKAC*α*) knockdown, but not PKA catalytic subunit *β* (PKAC*β*) knockdown, increases MYC. We show that the short term effect of pan-PKA inhibition on MYC is post-translational and the PKAC*α*-specific long term effect on MYC is transcriptional. These data also reveal distinct functional roles among PKA catalytic isoforms in MYC regulation. We attribute this effect to differential phosphorylation selectivity among PKA catalytic subunits, which we demonstrate for multiple substrates. Further, we also show that MYC up-regulates *PKACβ*, transcriptionally forming a proximate positive feedback loop. These results establish PKA as a regulator of MYC and highlight the distinct biological roles of the different PKA catalytic subunits.

MYC is a basic helix-loop-helix leucine zipper transcription factor that regulates a large number of target genes important in cell growth, metabolism, differentiation, proliferation, and apoptosis (1–6). Complete loss of MYC function results in embryonic lethality, whereas its overexpression predisposes cells to malignant transformation (7–9). MYC overexpression is an early and consistent feature of many human malignancies, where it is suspected to regulate key events in tumorigenesis.

Because MYC drives the transcription of genes important in multiple cellular processes, precise temporal regulation of MYC is required. Tight regulation of MYC is achieved through multiple mechanisms at the transcriptional, post-transcriptional, translational, and post-translational levels (10–14). Once translated, MYC is rapidly turned over in normal cells. The MYC steady-state level is regulated at the post-translational level through a series of exquisitely orchestrated phosphorylation events. Ras-mediated activation of MAPK stabilizes MYC by phosphorylation at Ser-62 within the evolutionarily conserved MYC box I region (11). Ser-62-phosphorylated MYC is recognized by GSK3*β*, which phosphorylates Ser-62-primed MYC at Thr-58. Peptidylprolyl isomerase 1 then catalyzes a *cis* to *trans* isomerization of the bond preceding Ser-62, thereby allowing the trans-specific protein phosphatase 2A to remove the stabilizing phosphorylation at Ser-62 (15, 16). MYC phosphorylated at Thr-58, but not Ser-62, is recognized by the E3 ligase Fbw7, which ubiquitinates MYC at the N terminus and targets it for proteasome-dependent degradation (11, 17). Recently, another E3 ligase, *β*trcp, was shown to interact through a previously unknown phospho-degron and oppose the Fbw7-mediated ubiquitination at the N terminus. PLK1[3] phosphorylation within the phospho-degron was reported to be critical for *β*trcp binding (18).

In this study, we demonstrate the existence of a MYC-PKA-PLK1 signaling loop and show that MYC is regulated both through transcriptional and post-translational mechanisms by PKA, in a PKA catalytic subunit isoform-specific manner. This work also highlights both the promise and potential pitfalls of global kinase inhibition and emphasizes the need to develop next generation therapeutic strategies capable of disrupting specific kinase-substrate interactions.

EXPERIMENTAL PROCEDURES

Antibodies, Reagents, and Vectors—Antibodies were as follows: c-MYC (N-term) (Epitomics, 1472-1); pan-PKA antibody (BD Biosciences, 610980); Thr-197 phospho-PKA (Cell Sig-

* This work was supported, in whole or in part, by National Institutes of Health Grant RCA155568A (to C. J. B.).
[S] This article contains supplemental Tables S1 and S2.
[1] Present address: Dept. of Molecular Biophysics and Biochemistry, Yale University, New Haven, CT.
[2] To whom correspondence should be addressed. E-mail: bieberic@umbc.edu.

[3] The abbreviations used are: PLK1, polo-like kinase 1; MBP-1, MYC promoter-binding protein 1, qRT, quantitative RT; RIKA, reverse in-gel kinase assay; TBP, TATA-binding protein.

naling, 4781S); HA antibody (Roche Applied Science, 11867423001); donkey anti-rabbit, donkey anti-mouse, and goat anti-rat HRP-linked (Jackson Laboratories). Reagents were as follows: H89 Insolution (Calbiochem), BI2536 (Selleck Chemicals, S1109), myristoylated PKI (14–22) amide (Biomol, P-210), and MG132 (Sigma). For vector constructs, all proteins purified from *Escherichia coli* were expressed using pQE80 vectors (Qiagen). The pCDNA3.1 vector (Invitrogen) was used for mammalian cell transfections.

Expression and Purification of Recombinant Proteins—All proteins were cloned with an N-terminal His_6 tag and expressed in either *E. coli* or mammalian cells (COS cells or PC3 cells). Recombinant proteins were purified under native conditions using Ni-affinity chromatography. The purified proteins were further enriched by ion-exchange chromatography whenever necessary. The final buffer condition for all proteins used in *in vitro* kinase assay is 50 mM NaH_2PO_4, 300 mM NaCl, 250 mM imidazole, and 0.1% Tween 20.

Cell Culture and Transfection—PC3, LNCaP, and 22RV1 cells (Invitrogen) were cultured in RPMI 1640 medium containing L-glutamine and supplemented with 10% heat-inactivated fetal bovine serum in 5% CO_2 at 37 °C. Cells were transfected using LipoD293 (SignaGen) according to the manufacturer's instructions. Lipofectamine 2000 (Invitrogen) was used to transfect siRNA as described previously (19, 20). The siRNA sequences used for PKACα knockdown are 5′-AAGCUCCCUUCAUACCAAAGU-3′ and 5′-ACUUUGGUAUGAAGGGAGCUU-3′. The siRNA sequences used for PKACβ knockdown are 5′-AAGGUCCGAUUCCCAUCCCAC-3′ and 5′-GUGGGAUGGGAAUCGGACCUU-3′.

Western Blotting and Immunoprecipitation—For Western blot analysis, mammalian cells were harvested 24–48 h post-transfection and lysed using 150 mM NaCl, 50 mM Tris (pH 7.5), 0.5% Nonidet P-40, and Complete protease inhibitor (Roche Applied Science). Western blotting was performed as described previously (21). Total protein from mouse prostate was extracted during RNA extraction using the protocol described in the RNeasy Kit (Qiagen). Western blotting was performed as described (22). PKACβ2 protein containing the N-terminal HA and His_6 tag was purified from transiently transfected COS and PC3 cells either by immunoprecipitation using an antibody against the HA tag or by Ni-affinity chromatography (further enriched by anion-exchange chromatography).

Quantitative PCR Analysis—Total RNA from mammalian cells was extracted using the RNeasy Kit (Qiagen) and reverse-transcribed using the Superscript cDNA synthesis kit (Bio-Rad). qRT-PCR was performed as per the instruction in the iScript qRT-PCR kit (Bio-Rad). -Fold difference in gene expression was determined after normalizing against GAPDH or TATA-binding protein (TBP) (as mentioned in the legends). Primers used for qRT-PCR are: MYC (134 bp), 5′-GCTCTCCTCGACGGAGTCC-3′ and 5′-CCACAGAAACAACATCGATTTCTT-3′; PKACβ(240 bp), 5′-TGGTGGGCATTAGGAG-3′ and 5′-CTTGTGAGTTTTTATATCACTGAC-3′; PKACβ2 (191 bp), 5′-AACCACCTTGTAACCAGTAT-3′ and 5′-TTTGGCTAGAAACTCTTTCA-3′; TBP (100 bp), 5′-GCCAGCTTCGGAGAGTTCTG-3′ and 5′-GCACGAAGTGCAATGGTCTTT-3′; GAPDH (226 bp), 5′-GAAGGTGAAGGTCGGAGT-3′ and 5′-GAAGATGGTGATGGGATTTC-3′.

In Vitro Kinase Assay—In vitro kinase assay was performed using purified recombinant proteins as described previously (21, 23). Kinase assay was carried out for 2 h at room temperature and stopped using 2× Laemmli buffer. After *in vitro* kinase assay, the proteins were analyzed by SDS-PAGE, transferred to a PVDF membrane, and analyzed by autoradiography. The PVDF membrane was also stained with Coomassie Brilliant Blue to reveal protein loading.

Reverse In-gel Kinase Assay (RIKA)—50 mg/ml PKACα in 8 M urea, 50 mM NaH_2PO_4, 300 mM NaCl, 250 mM imidazole, and 0.1% Tween 20 was co-polymerized in the gel, and RIKA was performed as described previously (23). RIKA was performed on a PVDF membrane for PLK1-priming experiments (on-membrane kinase assay). Purified recombinant MYC and MYC mutants were resolved by SDS-PAGE and transferred onto a PVDF membrane. The proteins on the membrane were refolded using the buffer conditions used in RIKA. The membrane was incubated with purified active recombinant PLK1 ($PLK1^{T210D}$) for 2 h in a buffer containing 20 mM Tris (pH 7.6), 20 mM $MgCl_2$, 50 mM DTT) and [γ-^{32}P]ATP. The membrane was washed with water overnight to remove nonspecifically bound ATP. Phosphorylation of MYC by PLK1 was detected by autoradiography.

Protein Identification and Phosphosite Mapping Mass Spectrometry—In-gel tryptic digestion was performed as described previously (23). Desalted tryptic peptides were analyzed by nano-LC-tandem MS on a linear ion-trap mass spectrometer (LTQ; Thermo Fisher). Acquired data were searched against a *Homo sapiens* protein database or phosphoproteome database using the TurboSEQUEST algorithm (Thermo Fisher).

Immunofluorescence—Cells were plated on poly-L-lysine-treated glass coverslips in 6-well plates. PC3 cells were grown on coverslips and transfected using lipoD293T (Signagen) according to the manufacturer's instructions. Transfected cells were fixed using 2% paraformaldehyde in PBS. Immunofluorescence analysis was performed as described previously (22).

RESULTS

PKA Activity Influences the Steady-state Levels of MYC—During our efforts to identify PKA substrates in prostate cancer cells, we identified α-enolase as a PKACα substrate (Table 1). An alternative in-frame internal translation initiating at +291 of the α-enolase mRNA yields an alternate product termed MYC promoter-binding protein 1 (MBP1) (24). We confirmed both ENO1 and MBP1 to be substrates of PKACα by *in vitro* kinase assay (Fig. 4*E*). Because MBP1 is a known transcriptional repressor of MYC, we sought to determine whether phosphorylation of MBP1 by PKA has an effect on MBP1 function and steady-state MYC level (25). We monitored changes in endogenous MYC level in prostate cancer cells treated with the PKA-selective small molecule inhibitor H89 by Western blotting. Pan-PKA inhibition using H89 resulted in decreased MYC accumulation in prostate cancer cells (Fig. 1*A*). This was found to be consistent in HeLa and K562 cells as well (Fig. 1*B*). Inhibition of PKA using the PKA-specific peptide inhibitor PKI also destabilized MYC (Fig. 1*C*). Conversely, activation of PKA

TABLE 1

PKACα substrates identified by mass spectrometry

PKA substrates identified by RIKA were excised from the gel, and protein identity was determined by mass spectrometry.

Protein name	Accession number	Rank	Mascot score	Peptides matched	Sequence coverage	Predicted mass *kDa/pI*	Known PKA substrate?
					%		
ATP synthase subunit β (ATPB)	P06576	1	124	14	38	56.5/5.2	No
Actin, cytoplasmic 1 (β-actin)	P60709	1	58	7	24	41.7/5.3	Yes
Triose phosphate isomerase I (TPI I)	P60174	1	153	12	63	26.6/6.4	No
Elongation factor 1δ	P29692	1	131	10	38	31.1/4.9	No
Hetrogeneous nuclear ribonucleoprotein H (hnRNP H)	P31943	2	90	9	21	49.1/5.8	No
40S ribosomal protein SA (p40)	P08865	1	70	9	38	32.8/4.7	No
Thyroid receptor-interacting protein 13 (TRIP-13)	Q15645	1	51	12	31	48.5/5.7	No
Ubiquitin carboxyl-terminal hydrolase isozyme L5 (UCHL5)	Q9Y5K5	1	59	19	52	37.5/5.2	No
Complement component 1Q subcomponent-binding protein	Q07021	1	65	6	38	31.3/4.7	No
Ubiquitin carboxyl-terminal Hydrolase isozyme L3 (UCHL3)	P15374	1	125	9	51	26.1/4.8	No
78-kDa glucose-regulated protein precursor (GRP 78)	P11021	1	155	15	26	72.2/5.0	No
T-complex protein 1 subunit θ	P50990	1	144	25	34	59.5/5.4	No
α-Enolase (ENO1)	P06733	1	81	24	54	47.1/7.0	No
Histone-binding protein (RBBP4)	Q09028	1	74	7	19	47.6/4.7	No
Peptidyl-prolyl *cis-trans* isomerase B precursor	P23284	1	148	12	52	22.7/9.3	No
Glucosidase 2 subunit β Precursor	P14314	1	72	10	21	59.3/4.3	No
Methyl-CpG-binding domain protein 4	Q95243	1	52	20	27	66/9.1	No
Histone H2B	CAB02545	1	NA[a]	15	NA[a]	13.9/10.3	Yes
Family with sequence similarity 82	EAW91638	1	85	10	35	31/6.21	No

[a] NA, not applicable.

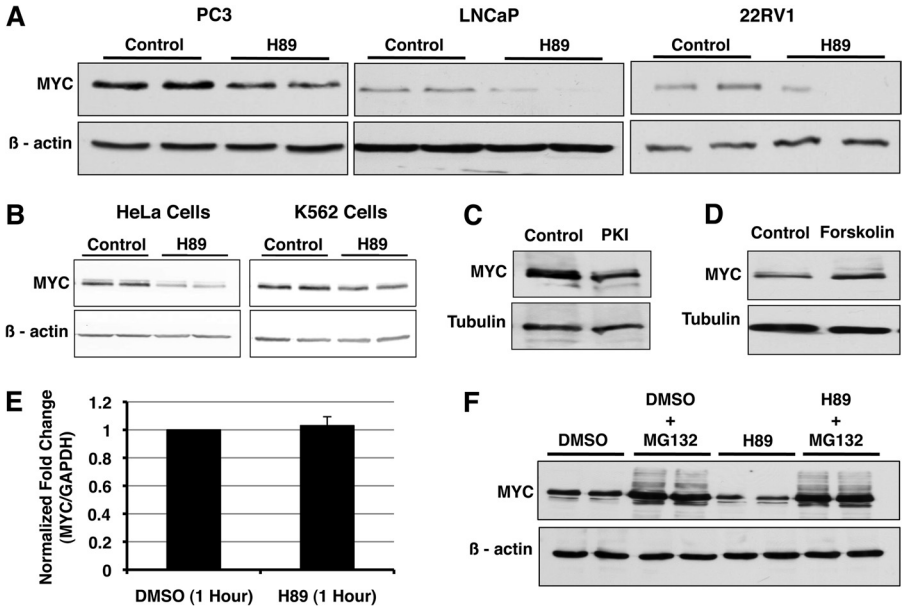

FIGURE 1. **PKA stabilizes MYC in cells.** *A* and *B*, PKA inhibition using H89 (10 mM, 1 h) decreased the MYC steady-state level in cells. *C*, PKA-specific peptide inhibitor PKI (20 mM, 1 h) destabilized MYC. *D*, PKA activation by forskolin (1 h) results in MYC accumulation. *E*, MYC mRNA level does not change upon H89 treatment ($n = 3$). *F*, PKA protects MYC from proteasome-mediated degradation. MG132 rescued the effect of PKA inhibition on MYC stability. *DMSO*, dimethyl sulfoxide.

using forskolin increased MYC levels (Fig. 1*D*). Although these results were consistent with our initial hypothesis, the rapid kinetics suggested that the effect could be the result of a direct interaction between PKA and MYC. To determine whether the effect of PKA on MYC is transcriptional, we evaluated changes in MYC mRNA levels upon PKA inhibition by qRT-PCR. The MYC mRNA level did not change upon H89 treatment, suggesting the effect of PKA inhibition on MYC to be post-transcriptional (Fig. 1*E*). Because MYC is degraded in cells via the 26S proteasome, we determined whether inhibition of proteasome activity rescues the effect of PKA inhibition on MYC accumulation. MG132 rescued the effect of PKA inhibition, thereby demonstrating that PKA protects MYC from 26S proteasome-mediated degradation (Fig. 1*F*).

MYC Phosphorylation at Ser-279 by PKA Stabilizes MYC—To determine whether PKA can phosphorylate MYC, we performed *in vitro* kinase reactions using recombinant PKACα and MYC in the presence of [γ-^{32}P]ATP. PKA efficiently phosphorylated MYC, and the phosphorylation was inhibited by H89 (Fig. 2, *A* and *C*). LC-MS^2 analysis identified Ser-279 as a

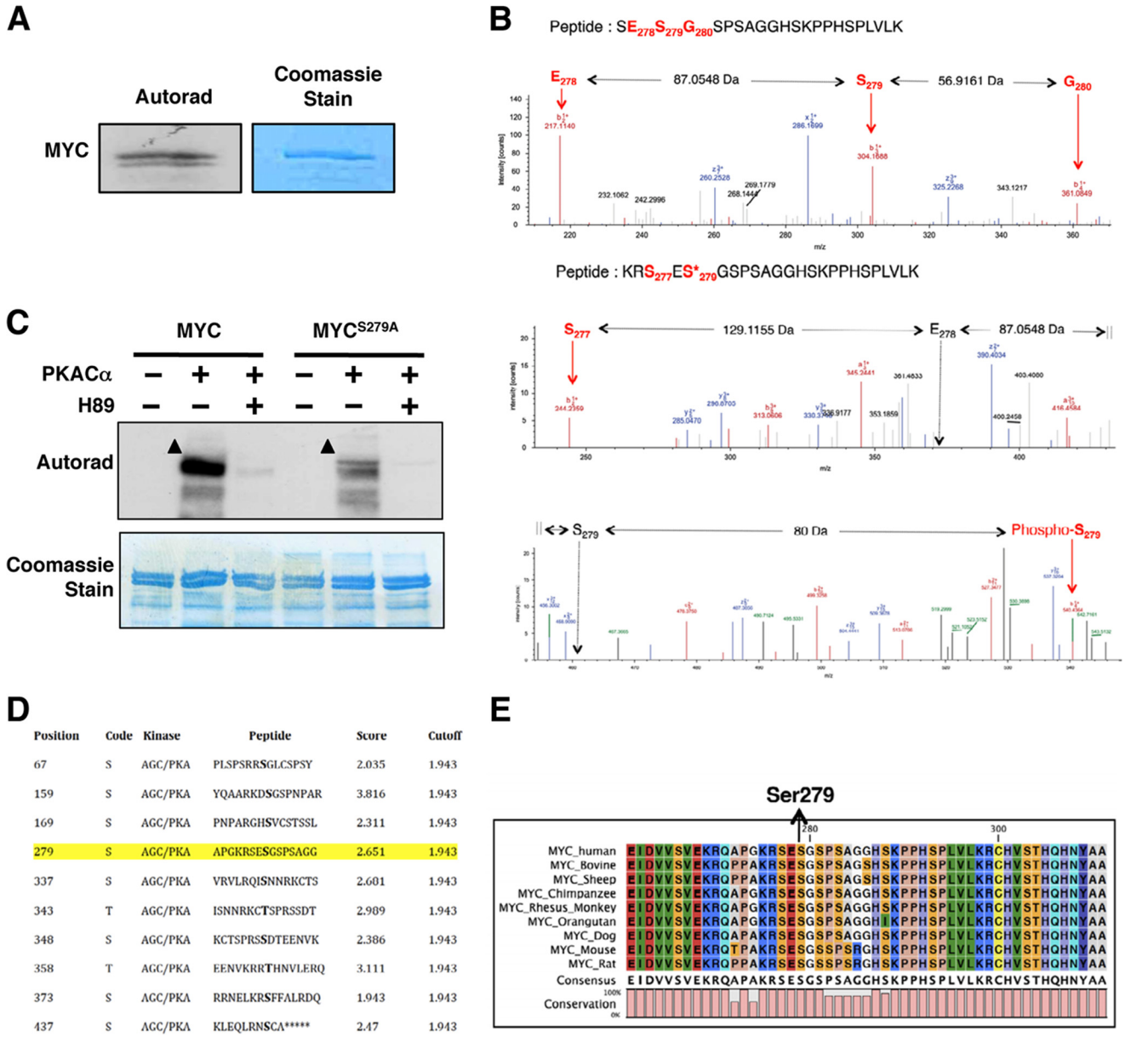

FIGURE 2. **PKA phosphorylates MYC at Ser-279.** *A*, PKACα phosphorylates MYC *in vitro*. *B*, PKACα phosphorylates MYC at Ser-279. *Top*, LC-MS^2 spectra of the peptide SESGSPSAGGHSKPPHSPLVLK from nonphosphorylated recombinant MYC are shown. A region spanning Ser-279 is shown to reveal the nonphosphorylated state at Ser-279. The *b* ions corresponding to Glu-278 and Ser-279 are labeled using *red arrows*. The corresponding amino acid in the peptide is also labeled in *red*. The mass difference between these ions is also indicated. A complete list of ions for the given peptide is listed in supplemental Table S1. *Bottom panels*, LC-MS^2 spectra of the peptide RSESGSPSAGGHSKPPHSPLVLK from PKA-phosphorylated recombinant MYC is shown. A region spanning Ser-279 is shown to reveal the phosphorylated state at Ser-279.The *b* ions corresponding to Ser-277 and phosphorylated Ser-279 (also designated by an *asterisk*) are labeled using a *red arrow*. The corresponding amino acid in the peptide is also labeled in *red*. The positions of the hypothetical Glu-278 and nonphosphorylated Ser-279 ion are indicated by the *black arrow*. The mass difference between these ions is also indicated. A mass increase of 80 Da was observed in the phosphorylated peptide, demonstrating that Ser-279 is phosphorylated. A complete list of ions for the given peptide is listed in supplemental Table S2. *C*, mutating Ser-279 to alanine diminished MYC phosphorylation by PKA *in vitro*. Addition of H89 completely abolished phosphorylation of MYC by PKA. *Arrowheads* indicate phosphorylated MYC. *D*, PKA phospho-acceptor sites on MYC are predicted by *in silico* phosphorylation prediction tool GPS 2.0 (43). Ser-279 is a predicted phospho-acceptor site of PKA on MYC (highlighted in *yellow*). *E*, the region containing Ser-279 in MYC is evolutionarily conserved across species.

PKA phospho-acceptor site on MYC (Fig. 2*B* and supplemental Tables S1 and S2). The ability of PKA to phosphorylate a MYC^{S279A} mutant *in vitro* was nearly extinguished compared with WT-MYC (MYC^{WT}), demonstrating Ser-279 as the major PKA phospho-acceptor site on MYC (Fig. 2*C*). Ser-279 is a predicted PKA phosphorylation site and is situated within an evolutionarily conserved region between the N-terminal transactivation and C-terminal DNA binding domains in MYC (Fig. 2, *D* and *E*). Furthermore, the region spanning Ser-279 is predicted to be solvent-exposed and intrinsically disordered (data not shown). Such intrinsically disordered domains have been implicated in the regulation of protein stability (26).

To determine whether the site phosphorylated by PKA on MYC is accessible and able to be phosphorylated *in vivo*, we transfected His_6-3×HA-tagged MYC in PC3 cells. The cells were harvested 36 h post-transfection, lysed (using 150 mM

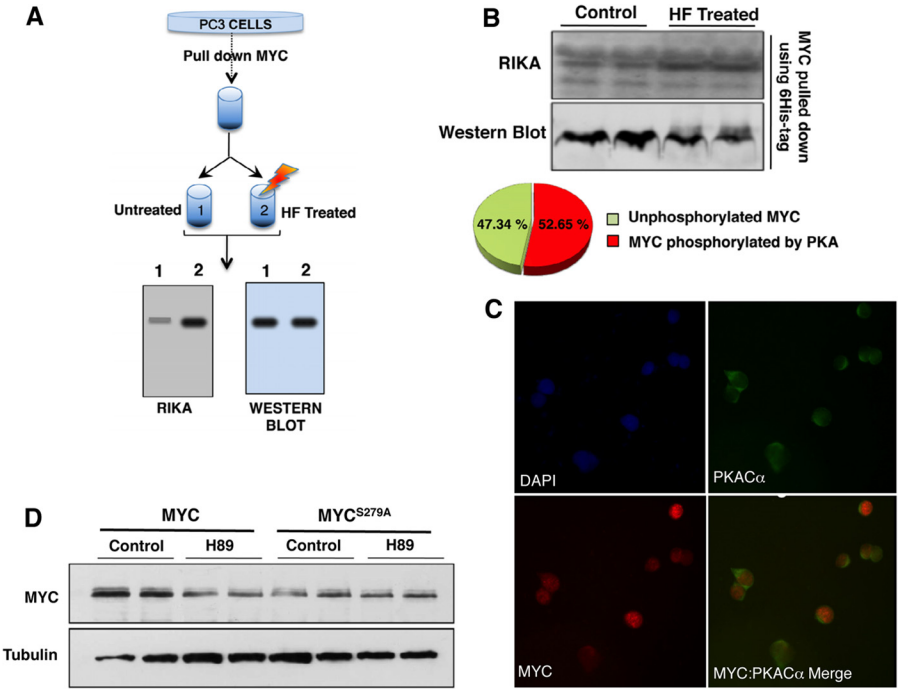

FIGURE 3. **PKA phosphorylation at Ser-279 stabilizes MYC.** *A*, scheme illustrates the RIKA-based approach used to determine whether the PKA phosphorylation site is phosphorylated *in vivo*. *B*, the PKA RIKA gel shows phosphorylation of untreated and HF-treated MYC purified from PC3 cells (*top*); Unphosphorylated MYC refers to the fraction of MYC not phosphorylated at a PKA site *in vivo* at the time of purification (*bottom*). A corresponding Western blot showing MYC levels (*bottom*) was used to normalize the phosphorylation signal on RIKA gel. *C*, immunofluorescence analysis co-localization of endogenous PKACα and MYC in PC3 cells is shown. *D*, ectopically expressed MYC^{WT} is destabilized upon PKA inhibition whereas MYC^{S279A} levels are not affected by H89. HA-tagged MYC^{WT} and MYC^{S279A} were transfected into PC3 cells. Anti-HA immunoblotting was performed to detect levels of transfected MYC following H89 treatment (20 μM, 1 h). Tubulin was used as loading control.

NaCl, 50 mM Tris (pH 7.5), 0.5% Nonidet P-40 and Complete protease inhibitor), and MYC was purified using Ni-affinity chromatography. The purified MYC was divided in half. One half was completely dephosphorylated by hydrogen fluoride (HF) treatment as described (27). The remaining half was left untreated and contained the pool of MYC molecules that retained their *in vivo* phosphorylation status. We performed a RIKA with PKA in the gel on the HF-treated and untreated purified MYC samples. If MYC is phosphorylated *in vivo* at the site phosphorylated by PKA *in vitro* (in a RIKA), then we would expect an increase in phosphorylation signal in the HF-treated samples (because these sites would be dephosphorylated upon HF treatment and become available to be phosphorylated during the RIKA). Total levels of MYC loaded in these samples were quantified by anti-HA Western blotting, and the change in phosphorylation signal was calculated after normalization as described previously (27). This process is illustrated in Fig. 3*A*. We observed ~50% increase in MYC phosphorylation upon HF treatment, suggesting that 50% of the *in vivo* MYC population in the cells was phosphorylated at the PKA site under the given culture conditions (Fig. 3*B*). Importantly, endogenous PKA and MYC co-localized to the nucleus (Fig. 3*C*).

To ascertain whether MYC phosphorylation at Ser-279 by PKA affected the MYC steady-state level, HA-tagged MYC^{WT} and MYC^{S279A} were transfected into PC3 cells, and the effect of PKA inhibition on their accumulation was analyzed. Whereas MYC^{WT} was destabilized upon H89 treatment, the steady-state level of MYC^{S279A} was unresponsive to PKA inhibition (Fig. 3*D*). Further, the MYC^{S279A} steady-state level was considerably lower compared with MYC^{WT} (Fig. 3*D*). These data demonstrate that phosphorylation at Ser-279 by PKA plays a role in stabilizing MYC in cells. No difference in subcellular localization between the endogenous MYC, HA-tagged MYC^{WT} and HA-tagged MYC^{S279A} mutant was observed (data not shown).

PKA Phosphorylation at Ser-279 Primes MYC for PLK1 Phosphorylation—A recent report showed the region spanning Ser-279 to constitute a phospho-degron (Fig. 4*A*). PLK1-mediated βtrcp binding within this region was shown to stabilize MYC (18). However, neither the events preceding PLK1 phosphorylation nor the PLK1 phospho-acceptor site(s) on MYC is known. Because both PLK1 and PKA phosphorylate residues within this phospho-degron, we sought to clarify their roles. We found that the effect of combined inhibition of PKA and PLK1 on MYC stability is more profound compared with inhibiting either kinase alone (Fig. 4*B*). We hypothesized three possible scenarios: (i) PKA and PLK1 phosphorylate the same residue on MYC (*i.e.* Ser-279) and hence elicit a similar response; (ii) PKA and PLK1 phosphorylate mutually independent residues on MYC within the phospho-degron; and (iii) PKA phosphorylates MYC at Ser-279, which primes PLK1 to phosphorylate an adjacent residue within the phospho-degron by relieving the inhibitory effect of the polo-box domain or by making an adjacent site a more favorable PLK1 phospho-acceptor (Fig. 4*C*). To distinguish among these models, we performed an *in vitro* kinase reaction using recombinant $PLK1^{T210D}$ and recombinant MYC, which was either prephosphorylated by PKA *in vitro* using nonradiolabeled ATP (primed) or not prephosphorylated by PKA (unprimed). His_6-tagged MYC purified from

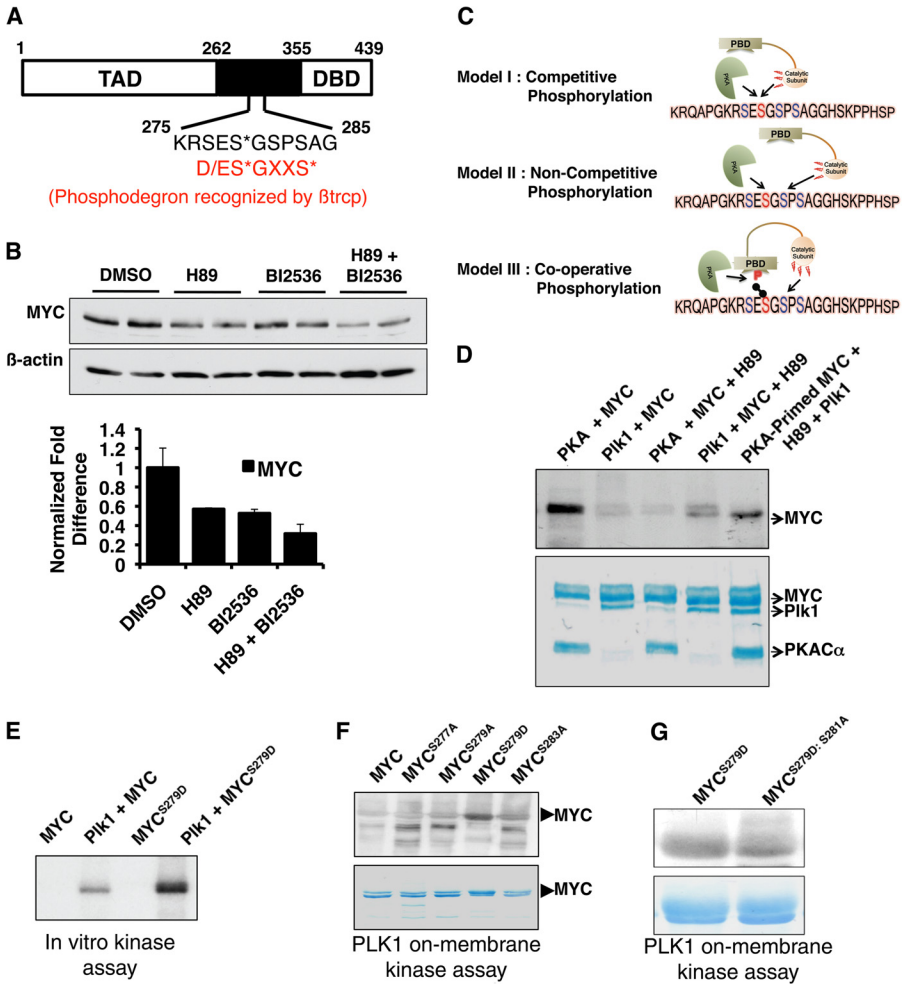

FIGURE 4. **PKA phosphorylation primes MYC for PLK1 phosphorylation.** *A*, Ser-279 lies within a phospho-degron region important in the stability of MYC. The canonical degron sequence (D/ES*G*XXS**) requires Ser-279 to be phosphorylated for efficient binding of the E3 ligase βtrcp (18). Phospho-acceptor sites within the phospho-degron are designated by *asterisks*. *TAD*, transcription activation domain *DBD*, DNA binding domain. *B*, inhibition of both PKA (20 μM H89, 3 h) and PLK1 (50 nM BI2536, 3 h) destabilized MYC. The effect of combined inhibition of PKA and PLK1 was more profound compared with inhibiting either kinase alone. Data from multiple experiments were quantified and are presented ± S.E. (*error bars*). *DMSO*, dimethyl sulfoxide. *C*, scheme illustrates the three possible mechanisms through which PKA and PLK1 could regulate MYC stability by phosphorylation within the phospho-degron. *D*, MYC phosphorylation by PKA primes phosphorylation by PLK1. Prephosphorylation of recombinant MYC by PKA (using nonradiolabeled ATP) prior to phosphorylation by PLK1 resulted in enhanced PLK1 phosphorylation (using [γ-^{32}P]ATP) (*top*). Addition of H89 completely blocks subsequent phosphorylation of MYC by PKA. Coomassie staining shows protein loading (*bottom*). *E*, *in vitro* kinase assay shows enhanced phosphorylation of MYC^{S279D} by PLK1 compared with MYC^{WT}. *F*, on-membrane kinase assay shows enhanced phosphorylation of MYC^{S279D} by PLK1 compared with MYC^{WT} and other MYC mutants. *G*, PLK1 phosphorylates MYC at Ser-281. PLK1 phosphorylation of MYC^{S279D} was diminished upon mutation of Ser-281 to alanine (MYC$^{S279D/S281A}$).

E. coli was prephosphorylated by *in vitro* kinase assay using recombinant PKACα and nonradiolabeled ATP. Nonphosphorylated MYC served as the unprimed control. Subsequently, H89 (30 μM), was added to all reactions to inhibit PKA activity. The absence of radiolabeling upon further incubation (1 h at room temperature) of the reactions containing MYC, PKA and H89 with [γ-^{32}P]ATP confirmed complete inactivation of PKA by H89. Recombinant PLK1^{T210D} and [γ-^{32}P]ATP was then added to these tubes containing either primed or unprimed MYC. The *in vitro* kinase reaction was allowed to proceed for 1 h at room temperature. Radioactive labeling of MYC by PLK1^{T210D} was assessed by running the reaction on a SDS-polyacrylamide gel, transferring to a PVDF membrane followed by autoradiography. We used the PLK1^{T210D} mutant version of PLK1 because it was previously shown to be constitutively active. The mutation at Thr-210 mimics the phosphorylation of PLK1 at this site within the activation loop, and phosphorylation at Thr-210 is necessary for PLK1 activation (28). We observed that the phosphorylation signal of MYC by PLK1^{T210D} (using [γ-^{32}P]ATP) was higher when MYC was primed by PKA (using nonradiolabeled ATP) compared with unprimed MYC (Fig. 4*D*). This result suggested that PKA phosphorylation at Ser-279 on MYC primes subsequent MYC phosphorylation by PLK1. To confirm this, we generated the phospho-mimetic mutant at Ser-279 (MYC^{S279D}) and performed an *in vitro* kinase assay using PLK1^{T210D}. We observed that PLK1 phosphorylation of the MYC^{S279D} mutant was dramatically higher compared with MYC^{WT} and other MYC mutants (Fig. 4*E*). We also compared the ability of PLK1^{T210D} to phosphorylate other MYC substitution mutants in the region and found MYC^{S279D} to be a more efficient PLK1 substrate compared with MYC^{WT} and other mutants (Fig. 4*F*). These results showed that MYC phosphorylation at Ser-279 increases the efficiency of subsequent PLK1^{T210D} phosphorylation of MYC, possibly at an adjacent

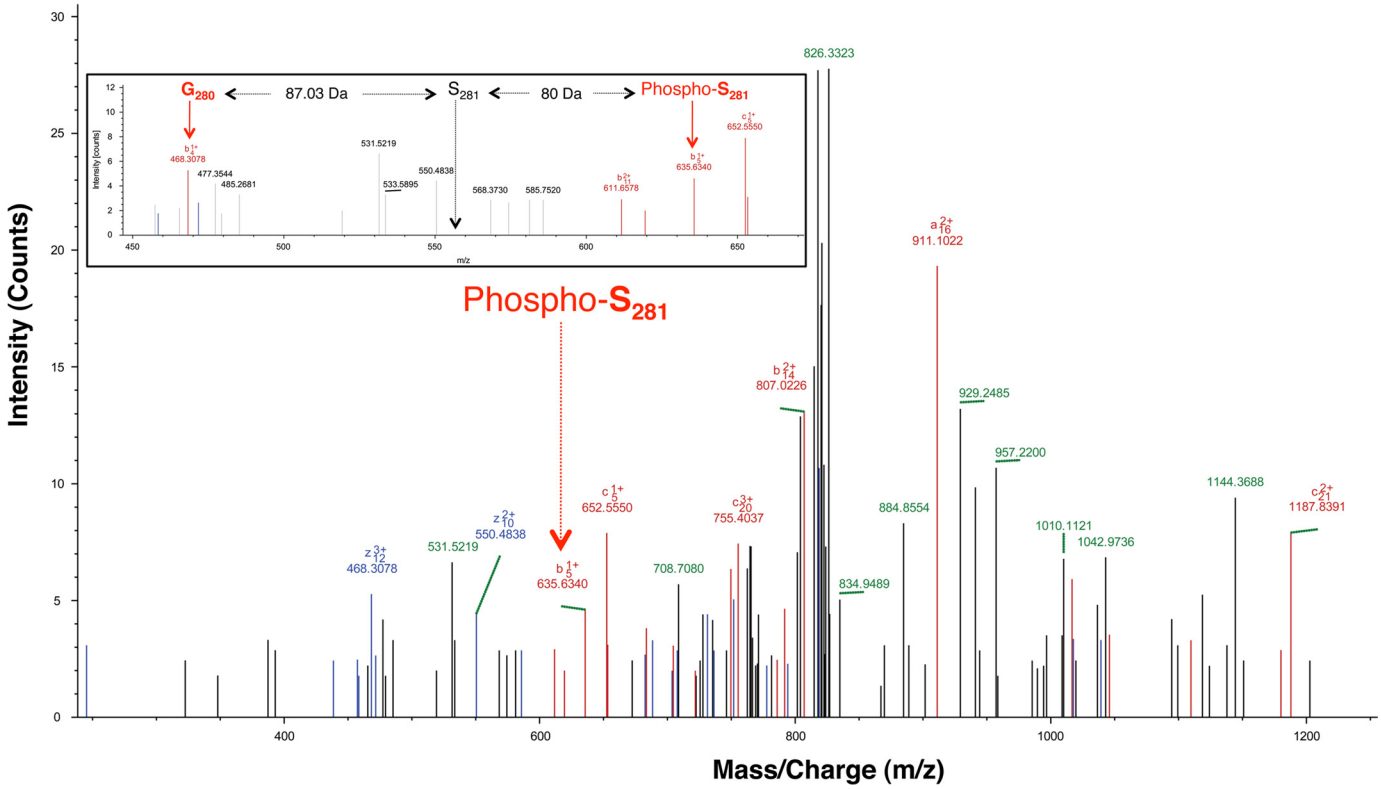

FIGURE 5. **PLK1 phosphorylates MYC at S281.** LC-MS^3 spectra of PLK1 phosphorylated MYC^{S279D}. The peak indicating phosphorylation at Ser-281 is indicated using a *red arrow*. *Inset*, LC-MS^3 spectra of the peptide RSEDGSPSAGGHSKPPHSPLVLK from PLK1 phosphorylated recombinant MYC. Region spanning Ser-281 is shown to reveal the phosphorylated state at Ser-281.The *b* ions corresponding to phosphorylated Ser-281 and Gly-280 are labeled using *red arrows*. The position of the hypothetical nonphosphorylated Ser-281 ion is indicated using a *black arrow*. The mass difference between these ions is also indicated. A mass increase of 80 Da was observed in the phosphorylated peptide, demonstrating that Ser-281 is phosphorylated.

site. LC-MS^3 analysis of MYC^{S279D} phosphorylated *in vitro* using PLK1^{T210D} revealed Ser-281 as the PLK1 phospho-acceptor site on MYC (Fig. 5). MYC^{S279D} phosphorylation by PLK1^{T210D} was significantly compromised in the MYCS$^{279D:S281A}$ double mutant (Fig. 4*G*), thus confirming Ser-281 as the major PLK1 phospho-acceptor site on MYC that is primed by Ser-279 phosphorylation.

PKA Isoform-specific Transcriptional Repression of MYC—Three different genes encode PKA catalytic subunits in humans: Cα, Cβ, and Cγ. The Cα and Cβ isoforms have multiple splice variants. To validate the effect of PKA inhibition on MYC and to dissect the role of individual PKA catalytic subunit isoforms in stabilizing MYC, we knocked down either PKACα or PKACβ using siRNA in PC3 cells. Analysis of siRNA-treated samples yielded an unexpected but intriguing result. Contrary to our expectation based on chemical PKA inhibition, knockdown of PKACα increased MYC steady-state level in PC3 cells (Fig. 6*A*). In contrast, PKACβ knockdown caused a slight decrease in MYC levels. Because siRNA knockdown occurs over an extended time period, we hypothesized that the result of PKACα knockdown on MYC could be through an indirect mechanism. Comparison of MYC mRNA after siRNA-mediated knockdown of PKA catalytic subunits revealed that prolonged knockdown of PKACα, but not PKACβ, increased the steady-state MYC mRNA level (Fig. 6*B*). These data reveal a link between PKACα activity and MYC transcription and, for the first time, show that the different PKA catalytic subunits perform distinct biological functions.

PKA Catalytic Subunit Isoforms Have Both Overlapping and Distinct Substrates—The ability of PKA catalytic subunits to have a distinct effect on the transcription of *MYC* suggested exclusive, nonredundant roles for PKA isoforms. We hypothesized that the different PKA catalytic subunit isoforms have distinct substrate profiles and hence elicit different responses upon activation. To test this hypothesis, we profiled and compared the substrates of PKA catalytic subunit isoforms by RIKA (23). To identify PKACα substrates, the PKACα RIKA was first standardized (Fig. 7*A*). LNCaP cell lysate was fractionated by anion-exchange chromatography, and a one-dimensional PKACα RIKA on the enriched fractions was performed to identify fractions containing PKA substrates (data not shown). Fractions containing PKACα substrates were used for two-dimensional PKACα RIKAs. The signal on RIKA gels was aligned with parallel silver-stained gels (Fig. 7*B*). PKA substrates were excised from the silver-stained gels and identified by mass spectrometry (Table 1). We validated a subset of the identified Cα substrates by *in vitro* kinase reaction using purified recombinant proteins (Fig. 7*C*).

To address whether substrate diversity contributes to the observed functional nonredundancy among PKA catalytic subunits, we tested the ability of PKACβ1 and PKACβ2 isoforms to phosphorylate these identified PKACα substrates *in vitro*. Cat-

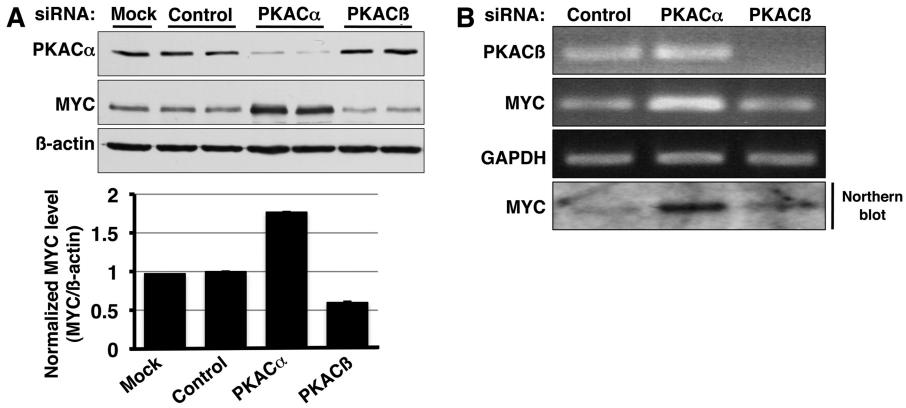

FIGURE 6. **PKA catalytic subunits regulate MYC differentially.** *A*, long term knockdown of PKACα by siRNA (48–72 h) resulted in increased MYC protein level whereas knockdown of PKACβ subunit caused a slight decrease in MYC protein level. Western blotting using pan-PKAC antibody confirmed knockdown of PKACα. PKACβ knockdown was confirmed by semiquantitative PCR (Fig. 6*B*). The change in MYC level was quantified using ImageJ software and normalized to the corresponding β-actin level. *B*, the effect of PKACα knockdown on MYC is transcriptional. Semiquantitative PCR and Northern blot analysis reveal an increase in MYC mRNA upon siRNA knockdown of PKACα but not PKACβ.

alytically active PKACβ2 was expressed and purified from mammalian cells (COS cells or PC3 cells) because PKACβ2 purified from *E. coli* was catalytically inactive (data not shown). We observed that whereas PKAβ1 phosphorylated all of the tested PKACα substrates (Fig. 7*D*), PKACβ2 phosphorylated only the telomerase-binding protein among the PKACα substrates tested (Fig. 7*E*). Addition of the pan-PKA inhibitor H89 diminished the phosphorylation of the telomerase-binding protein by PKACβ2 (Fig. 7*F*). These differences in substrate selectivity were not totally unexpected because PKACα and PKACβ1 share a very high sequence similarity (92%), whereas PKACβ2 has an additional 62 amino acids at its N terminus not present in PKACβ1 (Fig. 7*G*). *In silico* secondary structure prediction of PKACβ2 N terminus revealed an amphipathic helix region within this unique N terminus (Fig. 7*G*). We believe that this region might play a role in the differential substrate selectivity of PKACβ2.

Increased PKACβ Expression in MYC-overexpressing Prostate Epithelial Cells—PKACβ is known to be a direct transcriptional target of MYC in rat fibroblasts and lymphocytes (29). In these cells, it was further suggested that PKACβ plays an important role in MYC-mediated transformation (29). MYC overexpression is a consistent and key early event in prostate cancer, where it drives proliferation (30). Rapidly proliferating prostate epithelial cells have also been reported to have higher levels of the PKACβ2 isoform (31). These results prompted us to determine whether MYC overexpression in prostate cancer cells influences the PKACβ level (and the PKACβ2 splice variant), thereby forming a proximate positive feedback loop. Ectopic expression of MYC in PC3 cells resulted in increased PKACβ and PKACβ2 expression (Fig. 8*A*). We then compared the levels of PKACβ2 protein in the prostates of mice overexpressing MYC specifically in the prostate to their age-matched controls. We observed a positive correlation between MYC expression and PKCβ2 levels in the prostates of multiple mouse models in which MYC expression was controlled by distinct prostate-specific promoters (Fig. 8*B*). We could not compare levels of PKACβ1 protein in these experiments due to the unavailability of an antibody that would allow us to differentiate between the PKACβ1 and PKACα subunits, which have the same apparent molecular mass (~42 kDa). Oncomine analyses of previously published human prostate cancer microarray datasets revealed that both MYC and PKACβ are overexpressed in human prostate cancer cases (Fig. 8*C*) (32, 33). Oncomine analyses of multicancer datasets also revealed elevated PKACβ in prostate cancer (data not shown) (34, 35).

DISCUSSION

Diverse factors and signaling pathways influence MYC accumulation. In this study, we identified a role for PKA in MYC regulation and demonstrated the existence of a MYC-PKA-PLK1 signaling loop in cells. Our data show that MYC transcriptionally up-regulates PKACβ, and PKA in turn protects MYC from proteasome-mediated degradation through phosphorylation at Ser-279, establishing a proximate positive feedback interaction. Ser-279 lies within a phospho-degron recently shown to be important in MYC stability (18). These studies demonstrated this region to mediate binding of the E3 ligase βtrcp, which competes with Fbw7 (recruited through Thr-58 phosphorylation) for ubiquitination at the MYC N terminus (18). Phosphorylation within the degron was shown to be important for βtrcp recruitment, and PLK1 was suggested to phosphorylate MYC within this region (18). Our data demonstrate that MYC phosphorylation at Ser-279 by PKA primes subsequent PLK1 phosphorylation at Ser-281. Thus, through sequential phosphorylation, PKA and PLK1 cooperatively stabilize MYC.

Interestingly, whereas brief pharmacologic pan-PKA inhibition diminished MYC level, prolonged PKACα knockdown resulted in transcriptional up-regulation of MYC. These results provide an example of contrasting functional responses between short term and long term kinase inhibition. Furthermore, unlike in the case of PKACα knockdown, we observed no change in MYC mRNA level upon PKACβ knockdown, demonstrating functionally distinct roles for PKA catalytic isoforms in the transcriptional regulation of MYC. We hypothesized this transcriptional response to be mediated through a PKACα-specific substrate, possibly a transcription factor that regulates MYC transcription. Although the PKACα target(s) critical for

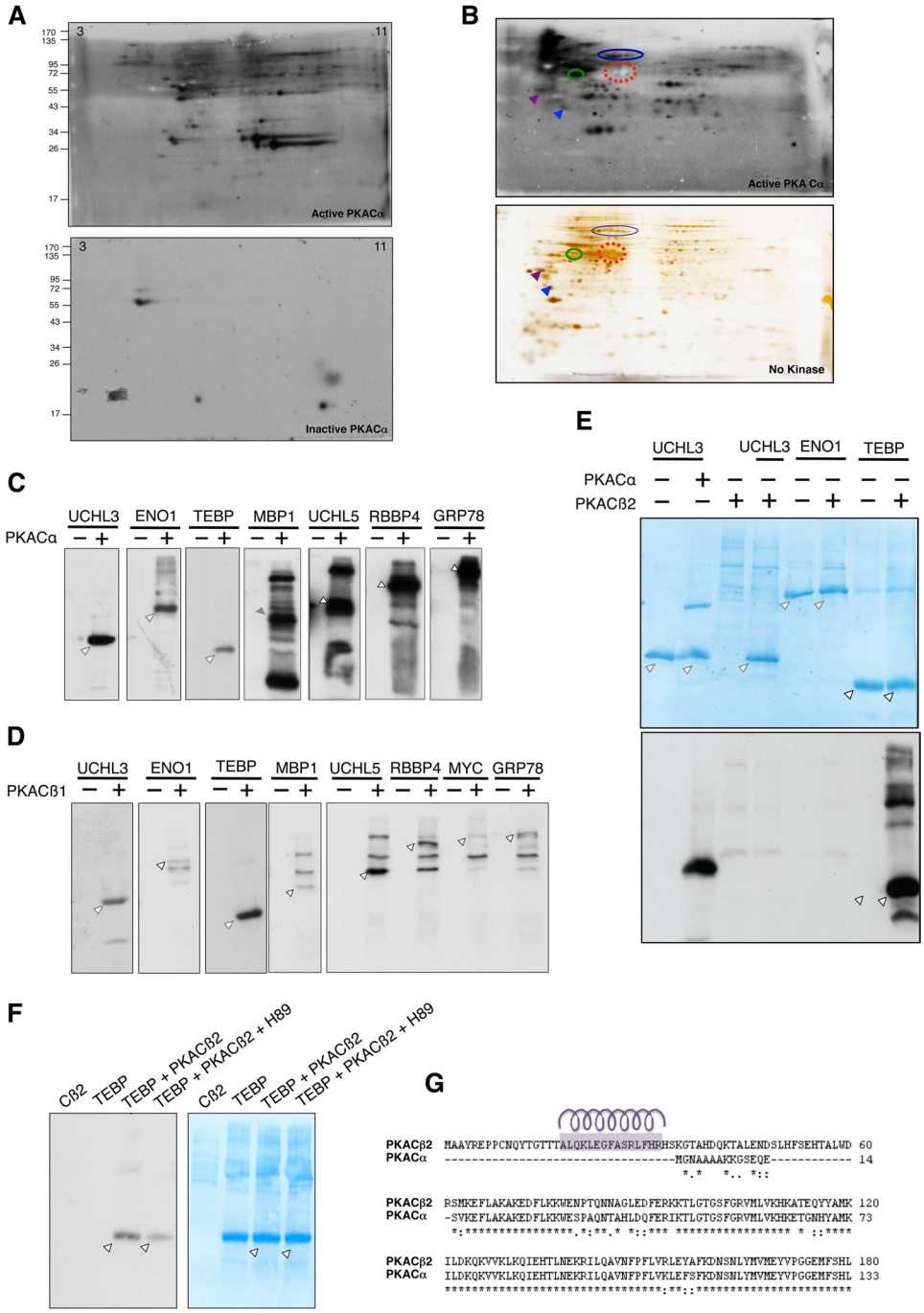

FIGURE 7. **PKA catalytic subunits have distinct substrate selectivity.** *A*, two-dimensional PKACα RIKA using an LNCaP whole-cell protein extract. *Numbers* on the *top left* and *right corners* indicate pH of the IPG strip. The autoradiograms from gel containing catalytically active PKACα (*top*) and the kinase-dead PKACα control (*bottom*) are shown. PKA substrates appear as signals on the autoradiograms. The signal on the control gel is likely due to autophosphorylation of endogenous kinases or phosphorylation of the co-polymerized kinase-dead PKACα or co-migrating proteins by endogenous kinases. *B*, two-dimensional RIKA on anion exchange fraction. A parallel gel from the same fraction (containing no kinase) was silver-stained to enable substrate identification (*bottom*). *Arrows* and *closed circles* represent several substrates used for alignment. *Red-dashed circle* represents an abundant non-PKACα substrate protein, which was used as an internal marker to align the gel. *C*, *in vitro* kinase assay using recombinant substrates and PKACα. Substrates identified by RIKA are phosphorylated by PKACα *in vitro*. *Arrowheads* indicate phosphorylated substrates. *D*, PKACβ1 has a substrate profile similar to that of PKACα. *In vitro* kinase assay was performed using recombinant PKACβ1 and PKACα substrates. PKACβ1 phosphorylated all tested PKACα substrates *in vitro*. *Arrowheads* indicate phosphorylated substrates. *E*, PKACβ2 has a distinct substrate profile compared with PKACα and PKACβ1. *F*, H89 inhibits phosphorylation of the telomerase-binding protein (*TEBP*) by PKACβ2. *G*, amino acid sequence alignment of N-terminal region PKACα and PKACβ2 shows the presence of an additional N-terminal arm (62 amino acids) in PKACβ2 isoform. The Yaspin secondary structure prediction program was used to predict the α-helical region in the N-terminal 62 amino acids in PKACβ2, and the helical wheel program available from the University of Virginia was used to reveal the amphipathic nature of the predicted helix region (indicated by *purple helix* over the corresponding sequence).

this response are unknown, CBP/p300 is a plausible candidate. Recruitment of CBP/p300 at the MYC promoter is known to down-regulate MYC transcription (36–38). CBP/p300 is a known PKACα substrate, but the effect of PKA phosphorylation on the DNA binding ability of CBP or recruitment to the MYC promoter region has not been investigated (39, 40). In this

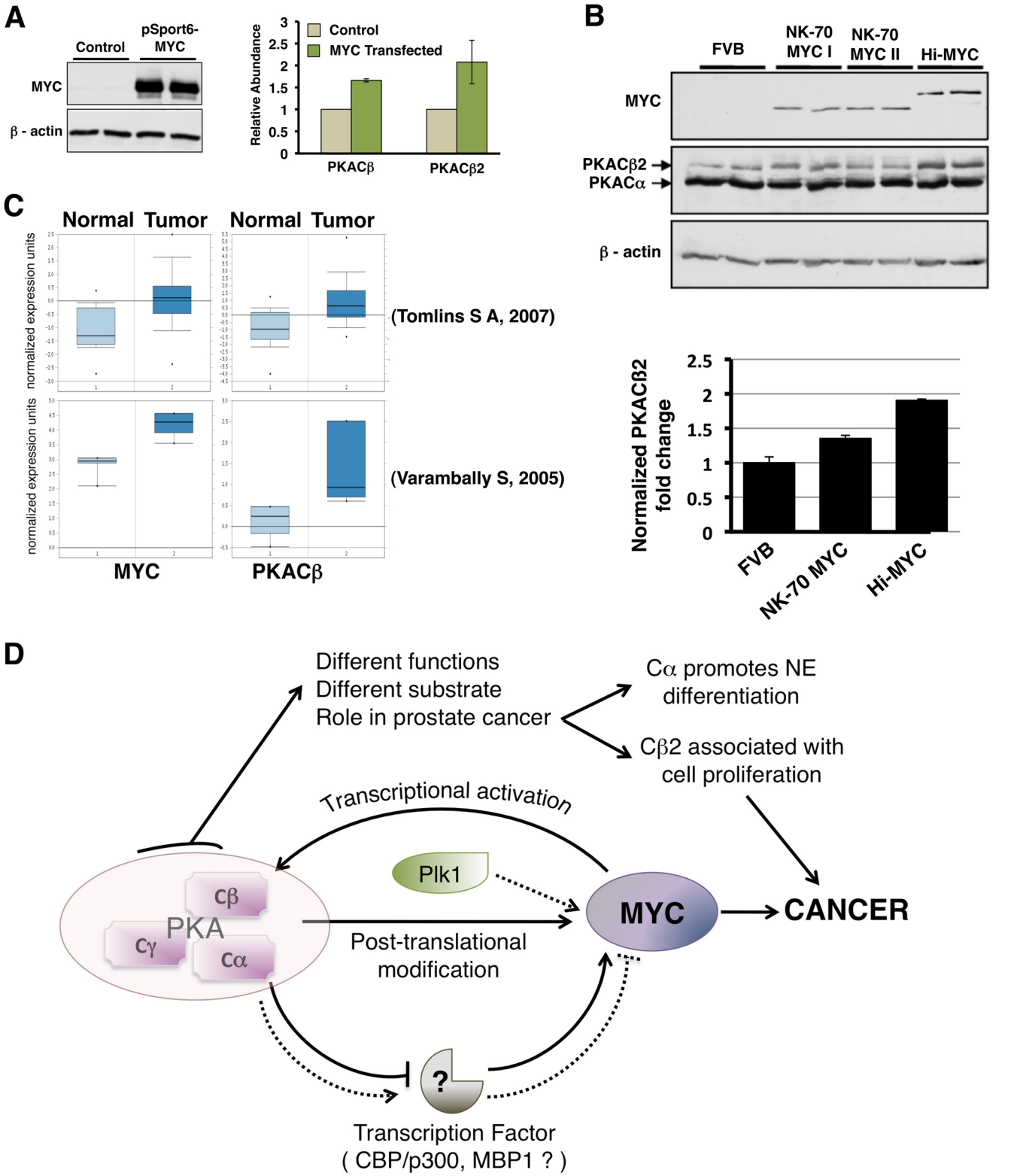

FIGURE 8. **MYC up-regulates *PKACβ* in prostate epithelial cells.** *A*, ectopic MYC expression in LNCaP cells (*left*), increasing Cβ and Cβ2 mRNA (*right*). Values are normalized to TBP mRNA level. *B*, comparison of Cβ2 protein level in the prostate of FVB and transgenic mice overexpressing MYC. Western blot analysis (*top*) of lysate from the prostate of age-matched FVB, Hi-MYC (MYC-driven using the *Probasin* promoter), and NK70-MYC (MYC driven by a 70-kb region of the *NKX3.1* promoter) reveal higher Cβ2 levels (47 kDa) in the prostate of MYC-overexpressing mice (*bottom*). *C*, Oncomine box plots comparing MYC, and PKACβ expression levels between normal and prostate cancer samples in multiple datasets (32, 33) show a positive correlation between levels of MYC and PKACβ in prostate cancer. *D*, MYC-PKA-PLK1 signaling loop. MYC positively regulates the level of the PKACβ isoform. Phosphorylation of MYC by PKA primes MYC for PLK1 phosphorylation. Together these phospho-transfer reactions stabilizes MYC. Prolonged knockdown of PKACα (but not PKACβ) transcriptionally up-regulates MYC. The different PKA catalytic subunits have distinct substrate specificity, which enables them to perform nonredundant functions.

regard, it will also be interesting to investigate the role of MBP-1 phosphorylation by PKA. During the course of this study we had identified MBP-1 as a PKACα (but not PKACβ2) substrate.

Comparison of substrate selectivity of the different PKA isoforms revealed PKACβ2 to have distinct phosphorylation selectivity compared with PKACα and PKACβ1. We attribute this difference to a predicted amphipathic helix in the N terminus of PKACβ2, which could mediate substrate recognition and binding. Except for this unique N terminus region, PKACβ2 is identical to PKACβ1, and PKACβ1 was shown to phosphorylate all PKACα substrates tested. Substrate docking domains distant from catalytic sites have been reported for multiple protein kinases (41). In addition, amphipathic helices have been reported to mediate several kinase-substrate interactions (42). We suggest that the solvent-exposed N-terminal amphipathic helix of PKACβ2 acts as a substrate-docking site and hence accounts for the differences in its substrate selectivity. These studies reveal the possibility of antithetical roles for closely related protein kinase isoforms and highlight the risk of therapeutic strategies aimed at global kinase inhibition. PKACα overexpression in LNCaP cells was reported to induce trans-differentiation of these cells into neuroendocrine-like cells, which divide slowly. It has also been reported that PKACβ2 is overexpressed in rapidly proliferating prostate cancer cells. Such discordance in the phenotype of cells overexpressing the different PKA isoforms argued for a significant functional difference between these proteins. The data reported here provide a mechanistic premise for the distinct functional roles of PKA catalytic subunits in prostate cancer. Although PKACα has been extensively studied and many of its substrates are known, the role of other PKA catalytic isoforms has received less attention. This report is the first detailed analysis of differences in substrate selectivity among PKA catalytic isoforms and the functional implications of these differences. Collectively, our data demonstrate that differential substrate selectivity and functional diversity among protein kinase isoforms are critical for modulation and precise signaling regulation in response to stimuli of varying intensity and perdurance.

Our model suggests that short PKA activity bursts in the cell stabilize MYC through a post-translational mechanism, whereas prolonged activation of PKACα transcriptionally represses MYC (Fig. 8*D*). This establishes a regulatory loop and protects the cells from downstream effects of post-translational MYC stabilization as a result of prolonged elevated PKACα activity. This mechanism could contribute to the slow proliferative rate of LNCaP cells trans-differentiated to a neuroendocrine-like phenotype by PKACα overexpression. MYC accumulation in turn activates a positive feedback loop that transcriptionally activates *PKACβ*. PKACβ protects MYC from proteasomal degradation, but does not repress MYC transcriptionally. This is consistent with the higher expression of PKACβ subunits in rapidly proliferating, MYC-overexpressing prostate cancer cells (31–33). Thus, through differential substrate selectivity, PKA catalytic isoforms regulate MYC differentially.

It is clear from the results presented here that the short and long term effects of PKA inhibition differ substantially. These observations underscore the need to establish kinase inhibition strategies that interfere with the ability of the kinase to interact with specific target substrates without impairing the function of the kinase in general. It may be possible to achieve this pharmacologically using peptides or peptidomimetics that interfere with interaction of protein kinases and specific substrates. Clearly, this strategy, which must be predicated upon an in-depth understanding of the structural aspects of kinase-substrate interactions, could enable subtle, yet functionally significant pathway disruption with fewer side effects and reduced toxicity compared with global inhibition strategies.

Acknowledgments—We thank Anu Divakaruni and Brandon McClary for technical assistance.

REFERENCES

1. Bernard, S., and Eilers, M. (2006) Control of cell proliferation and growth by Myc proteins. *Results Probl. Cell Differ.* **42,** 329–342
2. Dang, C. V. (1999) c-Myc target genes involved in cell growth, apoptosis, and metabolism. *Mol. Cell. Biol.* **19,** 1–11
3. Hoffman, B., and Liebermann, D. A. (2008) Apoptotic signaling by c-MYC. *Oncogene* **27,** 6462–6472
4. Jiang, G., Albihn, A., Tang, T., Tian, Z., and Henriksson, M. (2008) Role of Myc in differentiation and apoptosis in HL60 cells after exposure to arsenic trioxide or all-*trans*-retinoic acid. *Leuk. Res.* **32,** 297–307
5. Gao, P., Tchernyshyov, I., Chang, T. C., Lee, Y. S., Kita, K., Ochi, T., Zeller, K. I., De Marzo, A. M., Van Eyk, J. E., Mendell, J. T., and Dang, C. V. (2009) c-Myc suppression of miR-23a/b enhances mitochondrial glutaminase expression and glutamine metabolism. *Nature* **458,** 762–765
6. Schmidt, E. V. (1999) The role of c-myc in cellular growth control. *Oncogene* **18,** 2988–2996
7. Davis, A. C., Wims, M., Spotts, G. D., Hann, S. R., and Bradley, A. (1993) A null c-*myc* mutation causes lethality before 10.5 days of gestation in homozygotes and reduced fertility in heterozygous female mice. *Genes Dev.* **7,** 671–682
8. Lee, C. M., and Reddy, E. P. (1999) The v-*myc* oncogene. *Oncogene* **18,** 2997–3003
9. Ramsay, G. M., Moscovici, G., Moscovici, C., and Bishop, J. M. (1990) Neoplastic transformation and tumorigenesis by the human protooncogene MYC. *Proc. Natl. Acad. Sci. U.S.A.* **87,** 2102–2106
10. Dani, C., Blanchard, J. M., Piechaczyk, M., El Sabouty, S., Marty, L., and Jeanteur, P. (1984) Extreme instability of myc mRNA in normal and transformed human cells. *Proc. Natl. Acad. Sci. U.S.A.* **81,** 7046–7050
11. Sears, R. C. (2004) The life cycle of c-Myc: from synthesis to degradation. *Cell Cycle* **3,** 1133–1137
12. Lemm, I., and Ross, J. (2002) Regulation of c-myc mRNA decay by translational pausing in a coding region instability determinant. *Mol. Cell. Biol.* **22,** 3959–3969
13. Wall, M., Poortinga, G., Hannan, K. M., Pearson, R. B., Hannan, R. D., and McArthur, G. A. (2008) Translational control of c-MYC by rapamycin promotes terminal myeloid differentiation. *Blood* **112,** 2305–2317
14. Malempati, S., Tibbitts, D., Cunningham, M., Akkari, Y., Olson, S., Fan, G., and Sears, R. C. (2006) Aberrant stabilization of c-Myc protein in some lymphoblastic leukemias. *Leukemia* **20,** 1572–1581
15. Yeh, E., Cunningham, M., Arnold, H., Chasse, D., Monteith, T., Ivaldi, G., Hahn, W. C., Stukenberg, P. T., Shenolikar, S., Uchida, T., Counter, C. M., Nevins, J. R., Means, A. R., and Sears, R. (2004) A signalling pathway controlling c-Myc degradation that impacts oncogenic transformation of human cells. *Nat. Cell Biol.* **6,** 308–318
16. Arnold, H. K., and Sears, R. C. (2006) Protein phosphatase 2A regulatory subunit B56α associates with c-myc and negatively regulates c-myc accumulation. *Mol. Cell. Biol.* **26,** 2832–2844
17. Welcker, M., Orian, A., Jin, J., Grim, J. E., Grim, J. A., Harper, J. W., Eisenman, R. N., and Clurman, B. E. (2004) The Fbw7 tumor suppressor

regulates glycogen synthase kinase 3 phosphorylation-dependent c-Myc protein degradation. *Proc. Natl. Acad. Sci. U.S.A.* **101,** 9085–9090
18. Popov, N., Schülein, C., Jaenicke, L. A., and Eilers, M. (2010) Ubiquitylation of the amino terminus of Myc by SCF(β-TrCP) antagonizes SCF(Fbw7)-mediated turnover. *Nat. Cell Biol.* **12,** 973–981
19. Liu, J., Schuff-Werner, P., and Steiner, M. (2004) Double transfection improves small interfering RNA-induced thrombin receptor (PAR-1) gene silencing in DU 145 prostate cancer cells. *FEBS Lett.* **577,** 175–180
20. Amarzguioui, M. (2004) Improved siRNA-mediated silencing in refractory adherent cell lines by detachment and transfection in suspension. *BioTechniques* **36,** 766–768, 770
21. Padmanabhan, A., Gosc, E. B., and Bieberich, C. J. (2013) Stabilization of the prostate-specific tumor suppressor NKX3.1 by the oncogenic protein kinase Pim-1 in prostate cancer cells. *J. Cell. Biochem.* **114,** 1050–1057
22. Guan, B., Pungaliya, P., Li, X., Uquillas, C., Mutton, L. N., Rubin, E. H., and Bieberich, C. J. (2008) Ubiquitination by TOPORS regulates the prostate tumor suppressor NKX3.1. *J. Biol. Chem.* **283,** 4834–4840
23. Li, X., Guan, B., Srivastava, M. K., Padmanabhan, A., Hampton, B. S., and Bieberich, C. J. (2007) The reverse in-gel kinase assay to profile physiological kinase substrates. *Nat. Methods* **4,** 957–962
24. Feo, S., Arcuri, D., Piddini, E., Passantino, R., and Giallongo, A. (2000) ENO1 gene product binds to the c-myc promoter and acts as a transcriptional repressor: relationship with Myc promoter-binding protein 1 (MBP-1). *FEBS Lett.* **473,** 47–52
25. Chaudhary, D., and Miller, D. M. (1995) The c-myc promoter-binding protein (MBP-1) and TBP bind simultaneously in the minor groove of the c-myc P2 promoter. *Biochemistry* **34,** 3438–3445
26. Dyson, H. J., and Wright, P. E. (2005) Intrinsically unstructured proteins and their functions. *Nat. Rev. Mol. Cell Biol.* **6,** 197–208
27. Li, X., Rao, V., Jin, J., Guan, B., Anderes, K. L., and Bieberich, C. J. (2012) Identification and validation of inhibitor-responsive kinase substrates using a new paradigm to measure kinase-specific protein phosphorylation index. *J. Proteome Res.* **11,** 3637–3649
28. Smits, V. A., Klompmaker, R., Arnaud, L., Rijksen, G., Nigg, E. A., and Medema, R. H. (2000) Polo-like kinase-1 is a target of the DNA damage checkpoint. *Nat. Cell Biol.* **2,** 672–676
29. Wu, K. J., Mattioli, M., Morse, H. C., 3rd, and Dalla-Favera, R. (2002) c-MYC activates protein kinase A (PKA) by direct transcriptional activation of the PKA catalytic subunit β (PKA-Cβ) gene. *Oncogene* **21,** 7872–7882
30. Gurel, B., Iwata, T., Koh, C. M., Jenkins, R. B., Lan, F., Van Dang, C., Hicks, J. L., Morgan, J., Cornish, T. C., Sutcliffe, S., Isaacs, W. B., Luo, J., and De Marzo, A. M. (2008) Nuclear MYC protein overexpression is an early alteration in human prostate carcinogenesis. *Mod. Pathol.* **21,** 1156–1167
31. Kvissel, A. K., Ramberg, H., Eide, T., Svindland, A., Skålhegg, B. S., and Taskén, K. A. (2007) Androgen dependent regulation of protein kinase A subunits in prostate cancer cells. *Cell. Signal.* **19,** 401–409
32. Tomlins, S. A., Mehra, R., Rhodes, D. R., Cao, X., Wang, L., Dhanasekaran, S. M., Kalyana-Sundaram, S., Wei, J. T., Rubin, M. A., Pienta, K. J., Shah, R. B., and Chinnaiyan, A. M. (2007) Integrative molecular concept modeling of prostate cancer progression. *Nat. Genet.* **39,** 41–51
33. Varambally, S., Yu, J., Laxman, B., Rhodes, D. R., Mehra, R., Tomlins, S. A., Shah, R. B., Chandran, U., Monzon, F. A., Becich, M. J., Wei, J. T., Pienta, K. J., Ghosh, D., Rubin, M. A., and Chinnaiyan, A. M. (2005) Integrative genomic and proteomic analysis of prostate cancer reveals signatures of metastatic progression. *Cancer Cell* **8,** 393–406
34. Su, A. I., Welsh, J. B., Sapinoso, L. M., Kern, S. G., Dimitrov, P., Lapp, H., Schultz, P. G., Powell, S. M., Moskaluk, C. A., Frierson, H. F., Jr., and Hampton, G. M. (2001) Molecular classification of human carcinomas by use of gene expression signatures. *Cancer Res.* **61,** 7388–7393
35. Ramaswamy, S., Ross, K. N., Lander, E. S., and Golub, T. R. (2003) A molecular signature of metastasis in primary solid tumors. *Nat. Genet.* **33,** 49–54
36. Kolli, S., Buchmann, A. M., Williams, J., Weitzman, S., and Thimmapaya, B. (2001) Antisense-mediated depletion of p300 in human cells leads to premature G_1 exit and up-regulation of c-MYC. *Proc. Natl. Acad. Sci. U.S.A.* **98,** 4646–4651
37. Rajabi, H. N., Baluchamy, S., Kolli, S., Nag, A., Srinivas, R., Raychaudhuri, P., and Thimmapaya, B. (2005) Effects of depletion of CREB-binding protein on c-Myc regulation and cell cycle G_1-S transition. *J. Biol. Chem.* **280,** 361–374
38. Baluchamy, S., Sankar, N., Navaraj, A., Moran, E., and Thimmapaya, B. (2007) Relationship between E1A binding to cellular proteins, c-myc activation, and S-phase induction. *Oncogene* **26,** 781–787
39. Xu, L., Lavinsky, R. M., Dasen, J. S., Flynn, S. E., McInerney, E. M., Mullen, T. M., Heinzel, T., Szeto, D., Korzus, E., Kurokawa, R., Aggarwal, A. K., Rose, D. W., Glass, C. K., and Rosenfeld, M. G. (1998) Signal-specific co-activator domain requirements for Pit-1 activation. *Nature* **395,** 301–306
40. Swope, D. L., Mueller, C. L., and Chrivia, J. C. (1996) CREB-binding protein activates transcription through multiple domains. *J. Biol. Chem.* **271,** 28138–28145
41. Dimitri, C. A., Dowdle, W., MacKeigan, J. P., Blenis, J., and Murphy, L. O. (2005) Spatially separate docking sites on ERK2 regulate distinct signaling events *in vivo*. *Curr. Biol.* **15,** 1319–1324
42. Scott, J. W., Norman, D. G., Hawley, S. A., Kontogiannis, L., and Hardie, D. G. (2002) Protein kinase substrate recognition studied using the recombinant catalytic domain of AMP-activated protein kinase and a model substrate. *J. Mol. Biol.* **317,** 309–323
43. Xue, Y., Ren, J., Gao, X., Jin, C., Wen, L., and Yao, X. (2008) GPS 2.0, a tool to predict kinase-specific phosphorylation sites in hierarchy. *Mol. Cell. Proteomics* **7,** 1598–1608